Physica A 392 (2013) 271–277

Contents lists available at SciVerse ScienceDirect

Physica A

journal homepage: www.elsevier.com/locate/physa

Dynamics of snoring sounds and its connection with obstructive sleep apnea

Adriano M. Alencar [a,*], Diego Greatti Vaz da Silva [b], Carolina Beatriz Oliveira [b], André P. Vieira [a], Henrique T. Moriya [c], Geraldo Lorenzi-Filho [b]

[a] Instituto de Fisica, Universidade de São Paulo, SP, Brazil
[b] Sleep Laboratory, Pulmonary Division, Heart Institute (InCor), Faculty of Medicine, University of Sao Paulo, SP, Brazil
[c] Biomedical Engineering Laboratory of University of São Paulo, SP, Brazil

ARTICLE INFO

Article history:
Received 14 June 2012
Received in revised form 8 August 2012
Available online 25 August 2012

Keywords:
Snore
Hurst
Time interval
OSA

ABSTRACT

Snoring is extremely common in the general population and when irregular may indicate the presence of obstructive sleep apnea. We analyze the overnight sequence of wave packets — the snore sound — recorded during full polysomnography in patients referred to the Sleep Laboratory due to suspected obstructive sleep apnea. We hypothesize that irregular snore, with duration in the range between 10 and 100 s, correlates with respiratory obstructive events. We find that the number of irregular snores — easily accessible, and quantified by what we call the snore time interval index (STII) — is in good agreement with the well-known apnea–hypopnea index, which expresses the severity of obstructive sleep apnea and is extracted only from polysomnography. In addition, the Hurst analysis of the snore sound itself, which calculates the fluctuations in the signal as a function of time interval, is used to build a classifier that is able to distinguish between patients with no or mild apnea and patients with moderate or severe apnea.

1. Introduction

Temporal patterns of natural events can be used to detect hidden dynamics [1]. In fact, this connection dates back to Hurst's work [2] on the long-term memory (i.e. the autocorrelation) of a time series. This approach has been used to analyze respiratory sound events, and for instance the time interval between consecutive crackling sounds, generated when a collapsed airway opens, has been related to both lung structure and surface properties of the lung coating fluids [3,4]. The dynamics of various other physiological signals has been investigated with the help of tools derived from information theory and statistical mechanics (see e.g. [5,6] and references therein).

Snoring is perhaps the best known respiratory sound, and is characterized by a loud sound with frequency content between 20 and 300 Hz. It is caused by the vibration of soft tissues from the upper airway, including soft palate, uvula, tonsils, tonsilar pillars, base of tongue, lateral pharyngeal walls and mucous membranes [7]. Snoring occurs during sleep, when the pharyngeal muscles relax and may block the airway. Snoring is common in the general population, and does not necessarily indicate a disease. In contrast, irregular snoring is one of the hallmark signs suggestive of Obstructive Sleep Apnea (OSA). OSA is the most common sleep-disordered breathing, and is characterized by repetitive events of upper airway obstruction during sleep, causing total or partial cessation of airflow (apneas and hypopneas, respectively) [8].

* Corresponding author. Tel.: +55 11 3091 6658.
E-mail address: aalencar@if.usp.br (A.M. Alencar).

0378-4371/$ – see front matter © 2012 Elsevier B.V. All rights reserved.
doi:10.1016/j.physa.2012.08.008

A respiratory event is defined as apnea or hypopnea if its duration exceeds 10 s. Apnea is characterized by the cessation of airflow, while hypopnea is defined as a substantial reduction — of at least 50% — in airflow. OSA is a major public-health problem due to the high prevalence in the adult population (ranging from 4% to 10%), and due to the poor outcome when not recognized and treated. OSA is associated with recurrent asphyxia, fragmented sleep and generation of negative intrathoracic pressure during futile efforts to breath [9]. Although the patient is by and large unaware of these recurrent respiratory episodes during sleep, the consequences are multiple and may include excessive daytime sleepiness, fatigue, poor cognitive function and quality of life, as well as increased risk of motor vehicle accidents, metabolic and cardiovascular diseases. Full polysomnography is the gold standard method for OSA diagnosis, and the most important index expressing the severity of OSA is the apnea–hypopnea index (AHI), which is the average number of apnea or hypopnea events per hour. Sleep apnea is usually classified into mild, moderate or severe, depending on whether the AHI lies between 5 and 15 (mild), 15 and 30 (moderate), or above 30 events/h (severe) [10]. The major limitation of polysomnography is that it is an expensive and laborious test, which requires an overnight sleep in a specialized laboratory under the supervision of a sleep technician. Therefore, the development of alternative and simpler methods for the diagnosis of OSA is a priority [11].

Irregular snoring and witnessed apneas are the major signals indicating OSA and there is an increasing amount of research trying to relate OSA with snoring patterns. Most methods in the literature try to establish a correlation between OSA and either the number of snore events or the wave features of the snore such as intensity, sound frequency, number of snore events, spectral density, or a combination of these features [12–14]. Recently, Cavusoglu et al. [15,16] proposed the use of sequential properties of snoring episodes for OSA identification. They built sequences of snoring episode duration, snoring episode time separations and average snoring episode power, and were able to show that, using statistical properties of these sequences to measure snore regularity, OSA patients exhibit a greater degree of irregularity as compared with simple snorers. Following a related path, in this work we focus on the dynamics of irregular snoring episodes, and define a new Index, called the Snore Time Interval Index (STII), showing a strong positive correlation with the well-known apnea–hypopnea index. Furthermore, by a fluctuation analysis of the snore sound, through Hurst's R/S analysis, we build an automated classifier which is able to distinguish between patients with no or mild OSA and patients with moderate or severe OSA. In a similar spirit, a number of studies focused on the study of dynamic properties of sleep electroencephalogram (EEG) signals and their relation to OSA [17–19]. Here we work directly with acoustic signals, whose acquisition, in contrast with EEG signals, requires very simple equipment and no direct contact with the patients.

The remainder of this paper is organized as follows. In Section 2 we describe details regarding data acquisition and processing, and introduce the mathematical definitions used in this work. In Section 3 we present the results, and the paper ends in Section 4, in which we provide a discussion and our conclusions.

2. Methods

2.1. Experimental and pre-processing details

We analyzed snore records from patients referred to the sleep laboratory due to suspected OSA. The patients slept in a bed at the Sleep Laboratory of the Heart Institute at Clinics Hospital in São Paulo, Brazil, and we recorded the sounds in the room while the patients were simultaneously evaluated by a full polysomnography exam.

The population of 17 patients for which sound and polysomnography data are available was characterized by a male/female ratio of 11/6, average age 50 $\pm$ 10 years, average body mass index 30.7 $\pm$ 6.7 kg/m^2, and average apnea–hypopnea index 25.5 $\pm$ 22.5 events/h. Out of the 17 patients in the present study, 4 suffered from mild OSA, 6 from moderate OSA, and 7 from severe OSA.

The sound-recording system is based on a 16-bit audio codec (PCM 2901, Texas Instruments, USA) with a 4th order low-pass Butterworth analog filter (cutoff frequency of 5 kHz) and a 4th order high-pass Butterworth analog filter (cutoff frequency of 20 Hz). The audio codec is responsible for the acquisition (sampling frequency of 44.1 kHz) of the sound captured by the microphones, and the transmission of the recorded data to a laptop computer by a USB serial input. The sound was captured by two microphones located at the headboard of the bed, at a distance of 90 cm from each other.

The microphones acquired the sound $S(t)$ emitted by the patient plus the ambient noise, with a total time T, and recorded the data into a microcomputer for later analysis. Since the frequency content of the snore signal is predominantly between 20 and 300 Hz, the first step of the analyses was to digitally filter the signal, reducing the noise ratio. We found that the most suitable filter for dismissing the unwanted ambient noise while still keeping a strong snore signal was a 1024th-order band pass filter between 80 and 300 Hz.

Following the filtering, we square the filtered signal $S_f(t)$ and sum over all $[S_f(t)]^2$ in a time window Δt, with a window overlap of 50% between consecutive windows, building a new series of sound intensities I_m,

$$I_m = \sum_{t=\frac{m}{2}\Delta t}^{(\frac{m}{2}+1)\Delta t} [S_f(t)]^2, \tag{1}$$

with m going from zero to $2(T/\Delta t - 1)$, i.e., the series $\{I_m\}$ has a total of $2(T/\Delta t) - 1$ elements. We choose $\Delta t = 1$ s, since the normal breathing period is approximately 5 s, and we found that this discretization gives us a good overall precision for

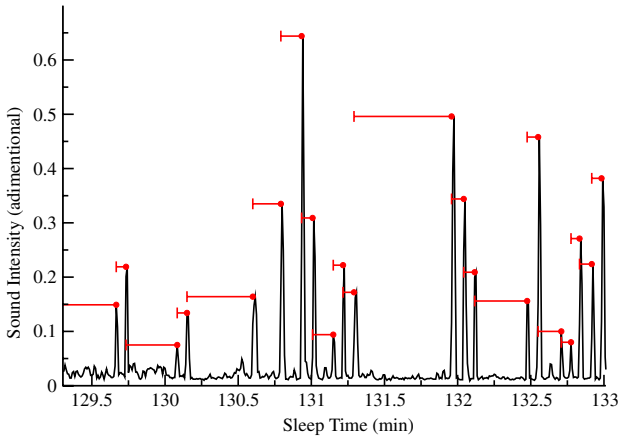

Fig. 1. Sound intensity versus time, showing the time intervals between consecutive detected snore events.

our study while keeping the signal less rough. We notice that the new series still exhibits considerable background noise, most of it coming from air-conditioning and electronic devices used by the Sleep Laboratory. From a region in the series without snore, we could determine a threshold I_0 below which all sounds are regarded as ambient noise, and then postulate that a group of points in our new series defines a single snore event when all I_m in the group lie above the threshold I_0. According to this definition, the jth snore event starts at point $m(j)$ and ends at the first point after $m(j)$ for which the corresponding intensity is less than I_0. Thus, in time units the jth snore event will start at $(1/2)\Delta t\, m(j)$. We then define the time interval between consecutive snores as the time from the beginning of one snore event to the beginning of the next one, $\delta t_j = (1/2)\Delta t\,(m(j) - m(j-1))$, as illustrated in Fig. 1.

At the moment, it is necessary to adjust the value of I_0 for each patient, considering the intensities of the snore and the ambient noise. We built a software program which is able to read the sound data and process the signal, giving us a log file containing the recording time in hours, minutes and seconds, and the average, median and standard deviation of the δt_j, as well as the maximum and minimum values of δt_j.

As breathing, snoring is an irregular phenomenon and it is an indicative of instability in the upper airways. Snore usually persists at each breathing cycle until one of three situations occurs: (i) the obstruction momentarily disappears; (ii) there is a partial collapse of the upper airways, restricting the airflow and leading to hypopnea; or (iii) the upper airway collapses, impairing the airflow and leading to an apnea event. We assume that in case (i) this momentary situation will persist for more than 100 s, and in both cases (ii) and (iii), after the patient restores normal breathing, (s)he will either get back to snoring or make a noise which will cross the ambient noise threshold I_0.

We then hypothesize that in a person that snores but does not have sleep apnea disorder, most snore time intervals δt will be less than 10 s or much larger than 100 s. On the other hand, for a patient with OSA we should find a lot of snore time intervals between 10 and 100 s, which in fact we found. Thus, in our analyses we focus on the range of time intervals δt between 10 and 100 s.

2.2. The snore time interval index

The apnea–hypopnea index (AHI) is the classical index to determine if a person has sleep apnea, and is only fully characterized when a person spends a night of sleep in a sleep laboratory wired with electrodes and using an air mask to measure air flow. Along the night a specialist medical doctor goes through the data and manually counts the number of apnea and hypopnea events N_{AH} occurring during the whole night. The AHI index is then evaluated as

$$AHI = N_{AH}/T, \tag{2}$$

where T is the number of sleep hours.

From the time intervals δt, defined in the previous subsection, we introduce what we call the Snore Time Interval Index (STII), which is related to the number $N_{\delta t}$ of snore time intervals for which 10 s $< \delta t <$ 100 s, being explicitly calculated as

$$STII = N_{\delta t}/T. \tag{3}$$

As we will show in Section 3, there is a strong positive correlation between AHI and STII.

2.3. A classifier based on Hurst's R/S analysis

Along the lines of Ref. [20], we also built an automated classifier from a fluctuation analysis of the intensities I_m, based on Hurst's R/S method (see e.g. [21]), which was introduced as a means of measuring memory effects in a time series.

The R/S method involves dividing a time series into intervals of size τ, within which a rescaled range is calculated as follows. For the kth interval, which we denote by L_k, we first determine the average of the time series,

$$z_{\tau,k} = \frac{1}{\tau}\sum_{m\in L_k} I_m, \tag{4}$$

which is used to define a cumulative deviation as

$$Z_{m,k} = \sum_{j=\ell_k}^{m}(I_j - z_{\tau,k}), \tag{5}$$

ℓ_k labeling the left end of L_k. From this cumulative deviation, we then extract a range,

$$R_{\tau,k} = \max_{m\in L_k} Z_{m,k} - \min_{m\in L_k} Z_{m,k}, \tag{6}$$

which is divided by the standard deviation of the original series,

$$S_{\tau,k} = \sqrt{\frac{1}{\tau}\sum_{m\in L_k}(I_m - z_{\tau,k})^2}, \tag{7}$$

to yield the rescaled range $R_{\tau,k}/S_{\tau,k}$ of a single interval. Repeating this procedure for all intervals L_k, we obtain the average rescaled range

$$\rho(\tau) = \frac{1}{n_\tau}\sum_{k}\frac{R_{\tau,k}}{S_{\tau,k}}, \tag{8}$$

where n_τ denotes the number of nonoverlapping intervals of size τ that can be fit into the original series.

When applied to a time series generated by a single dynamics, such as in fractional Brownian motion, the rescaled-range analysis yields a function $\rho(\tau)$ following a power-law with a so-called Hurst exponent H, which gauges memory effects on the dynamics. Different values of H indicate different underlying dynamics, and this has been used in a number of situations to distinguish between the systems producing the time series. Specifically, this approach can differentiate between healthy and diseased subjects as regards cardiac [22], neurological [23,24], and respiratory function [25]. However, as shown in the next section, this characterization in terms of a single parameter (the Hurst exponent) fails in the case of OSA, but the $\rho(\tau)$ curves still hide useful information about the patients' conditions. In order to extract that information, we resort to pattern-classification tools.

Given a set $\{\tau_j\} = \{\tau_1, \tau_2, \ldots, \tau_d\}$ of choices for the interval size τ, the corresponding set $\rho(\tau)$ measures the average relative fluctuation of the time series as a function of τ, and this can be seen as a vector in a multidimensional space,

$$\mathbf{x} = (\rho(\tau_1), \rho(\tau_2), \ldots, \rho(\tau_d))^t,$$

in which t indicates the vector transpose. The set of all vectors obtained by the R/S analysis can then be fed into standard algorithms from the pattern classification literature. Here, we employ a variant of the Karhunen–Loève (KL) transformation (see Ref. [26]), which can be seen as an improvement over principal-component analysis, implementing supervision and relying on the compression of discriminatory information contained in the class means.

In order to build a classifier whose performance is statistically significant, we split the intensity signals from each patient into subsignals containing 1024 points (corresponding to 512 s, an amount of time during which many snore events can happen), obtaining a total of 936 subsignals for all patients. The R/S analysis was performed for values of the time window τ corresponding to the nearest integers obtained from the powers of $2^{1/4}$ from 4 to 1024 points (with a total of 33 values).

The first step of the KL transformation involves projecting the feature vectors $\mathbf{x}_i$ (i labelling the vectors obtained from different sound samples) onto the eigenvectors of the within-class covariance matrix $\mathbf{S}_W$, defined by

$$\mathbf{S}_W = \frac{1}{N}\sum_{k=1}^{N_C}\sum_{i=1}^{N_k} y_{ik}(\mathbf{x}_i - \mathbf{m}_k)(\mathbf{x}_i - \mathbf{m}_k)^T, \tag{9}$$

where N_C is the number of different classes, N_k is the number of vectors in class k, and $\mathbf{m}_k$ is the average vector of class k. The element y_{ik} is equal to one if $\mathbf{x}_i$ belongs to class k, and zero otherwise. The resulting vectors are then rescaled by a diagonal matrix built from the eigenvalues λ_j of $\mathbf{S}_W$. In matrix notation, this operation can be written as

$$\mathbf{X}' = \mathbf{\Lambda}^{-\frac{1}{2}}\mathbf{U}^T\mathbf{X}, \tag{10}$$

in which $\mathbf{X}$ is the matrix whose columns are the training vectors $\mathbf{x}_i$, $\mathbf{\Lambda} = \mathrm{diag}(\lambda_1, \lambda_2, \ldots)$, and $\mathbf{U}$ is the matrix whose columns are the eigenvectors of $\mathbf{S}_W$. Finally, the resulting vectors are projected onto the eigenvectors of the between-class covariance matrix $\mathbf{S}_B$,

$$\mathbf{S}_B = \sum_{k=1}^{N_C}\frac{N_k}{N}(\mathbf{m}_k - \mathbf{m})(\mathbf{m}_k - \mathbf{m})^T, \tag{11}$$

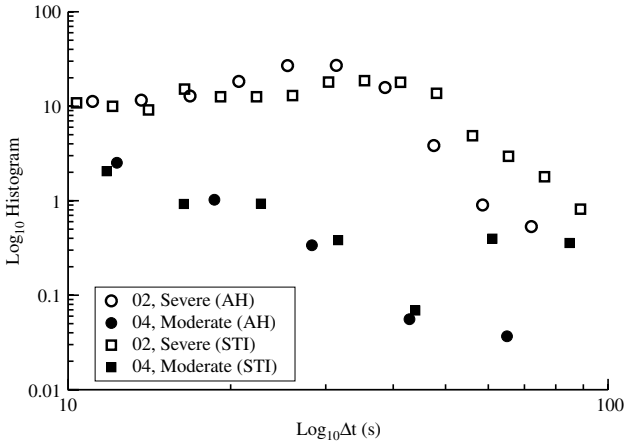

Fig. 2. The histogram of time intervals Δt between consecutive snores (square) and the histogram of apnea–hypopneia duration (circles) in seconds. We compare two extreme cases, filled and open symbols respectively for moderate and severe OSA.

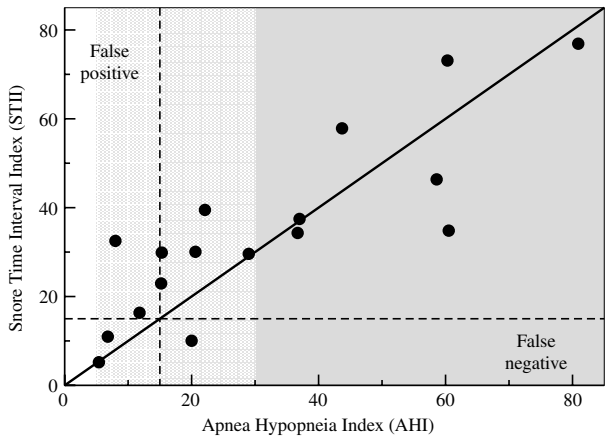

Fig. 3. Snore time interval index versus apnea–hypopneia index (AHI), the latter defined by the polysomnography for 17 patients. The straight line is a line with slope 1 to highlight the correlation between the two indexes (correlation coefficient of 0.841, with significance $t = 6.02$, indicating a probability of less than 0.1% for the null hypothesis of uncorrelated data). As defined by the AHI value, the dark gray region corresponds to severe OSA, the light gray region to moderate OSA, the lightest gray region to mild OSA, and the white region to normality. The dashed lines delimit the boundaries of the regions where the STII leads to false positive (upper left rectangle) or false negative (lower right rectangle) results, according to the classification in no/mild versus moderate/severe OSA.

where $\mathbf{m}$ is the overall average vector. The full transformation can be written as

$$\mathbf{X}'' = \mathbf{V}^T \Lambda^{-\frac{1}{2}} \mathbf{U}^T \mathbf{X}. \tag{12}$$

$\mathbf{V}$ being the matrix whose columns are the eigenvectors of $\mathbf{S}_B$ (calculated from $\mathbf{X}'$).

3. Results

As shown in Fig. 2, there is a remarkable agreement between the histogram of the duration of apnea or hypopnea events and the histogram of snore time intervals. Moreover, our results reveal a strong positive correlation between the apnea–hypopnea index and the snore time interval index, as depicted in Fig. 3. Notice that, assuming a perfect correlation between AHI and STII when it comes to classifying OSA into no/mild versus moderate/severe, the STII yields only one false negative and two false positive results (false positives being usually more tolerable mistakes).

Fig. 4 shows examples of curves obtained by Hurst's R/S analysis of sound samples taken from four different patients. Estimates of the Hurst exponents of the different curves for all patients, obtained by linear fits of the log–log curves, yielded results ranging between 0.7 and 0.8, with no significance correlation to the patients' condition. As described in the previous section, the Hurst curves, interpreted as feature vectors, were then fed into the automated classifier based on the KL transformation. The classifier was trained to recognize feature vectors of sound samples coming from two categories: (a) patients with no or mild OSA; and (b) patients suffering from moderate or severe OSA. The training was performed by

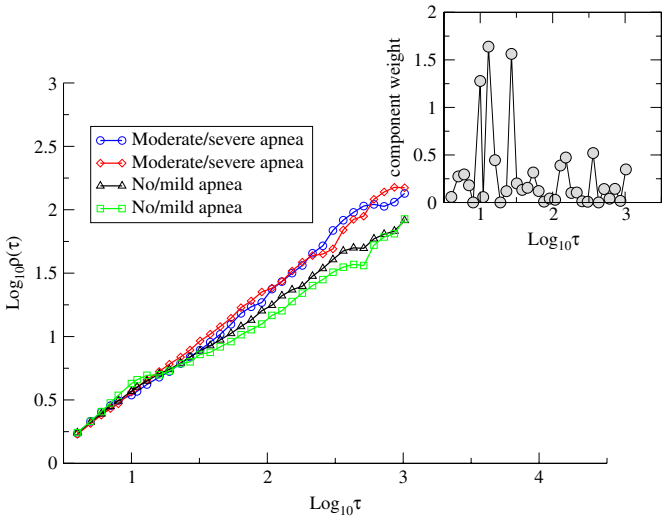

Fig. 4. Main plot: examples of curves obtained by Hurst's R/S analysis of the snore sounds, corresponding to the average relative fluctuation of the signal, ρ, versus the size of the time window, τ, in double-logarithmic scale. Sound samples from 4 different patients were used, two with no or mild apnea, and two with moderate or severe apnea. Inset: weights of the components of the Karhunen–Loève transformation vector corresponding to the different sizes of the time window. Projection of the fluctuation vector of a given sound sample onto the Karhunen–Loève vector determines the class to which the sample is attributed.

randomly selecting 748 out of the available 936 subsignals (about 80% of the total), and using the remaining signals for testing. During the training step, the mean transformed vectors of each class are extracted, and the (transformed) testing vectors are assigned to the class corresponding to the nearest mean transformed vector. With only two possible classes, the transformation matrix effectively reduces to a single line, i.e. a transformation vector.[1] The inset in Fig. 4 shows, for a typical transformation vector, the (unnormalized) weights of the components corresponding to different sizes of the time window. The peaks in the curve indicate those components which are most relevant for the decision process. Notice the existence of large peaks around $\tau = 20$ ($\log \tau \simeq 1.3$), corresponding to a time interval of 10 s, a time interval characteristic of many snore events in patients suffering from OSA.

This procedure was repeated for 100 distinct choices of training and testing vectors. Based on each subsignal individually, the average classification error during the testing step was 37% for category (a) and 28% for category (b). However, if one extracts a classification from a majority rule of the corresponding results for all subsignals belonging to a given patient, 16 of the 17 patients are correctly assigned to their respective categories. Interestingly, the misclassified patient has an AHI of 15.2, and thus lies on the borderline between categories.

4. Conclusions

To summarize, in the present study we propose a simple and accurate method to identify OSA based on the time intervals between snore events, and the average number of snore events per unit time, as revealed by the intensity of the sound. Our method of analyzing snore correlated remarkably well with the AHI derived from polysomnography, which is the gold standard method for OSA diagnosis. Moreover, an automated classifier based on the R/S analysis of the snore intensities was able to correctly identify patients with moderate to severe OSA.

Of course, our study has some limitations. Firstly, we tested this algorithm in a relatively small sample of patients referred to the Sleep Laboratory under controlled conditions. We have no means to predict at this stage how this method will perform in other settings and populations. However, it must be stressed that the physical conditions of the laboratory are probably similar to most bedrooms. We acknowledge that due to the simplicity of our snore detection scheme, some snore events may not be detected or some loud sound may be detected as a snore. However, these false or undetected snore events are expected to represent a small fraction of all events, and thus will be washed out in the statistics. We predict that more sophisticated methods to detect snores may improve the snore time interval index. Nevertheless, our work represents a first step towards establishing guidelines for snore classification and revealing a correlation between snoring events suspected of sleep-disordered breathing and the AHI, goals manifested in a recent medical review on the acoustics of snoring [27].

[1] This is a consequence of the fact that the subspace defined by the relative positions of the average vectors of the two classes, entering the definition of $\mathbf{S}_B$ in (11), is one-dimensional.

Acknowledgments

This work was supported by Fundação de Amparo à Pesquisa do Estado de São Paulo (FAPESP) and Conselho Nacional de Desenvolvimento Científico e Tecnológico (CNPq).

References

[1] N. Vandewalle, J.F. Lentz, S. Dorbolo, F. Brisbois, Avalanches of popping bubbles in collapsing foams, Phys. Rev. Lett. 86 (2001) 179.
[2] H.E. Hurst, Long-term storage capacity of reservoirs, Trans. Am. Soc. Civ. Eng. 116 (1951) 770–799.
[3] A.M. Alencar, S.V. Buldyrev, A. Majumdar, H.E. Stanley, B. Suki, Avalanche dynamics of crackle sound, Phys. Rev. Lett. 87 (2001) 088101.
[4] A.M. Alencar, S.V. Buldyrev, A. Majumdar, H.E. Stanley, B. Suki, Relation between crackle sound and the perimeter growth of a cayley tree: application to lung inflation, Phys. Rev. E 68 (2003) 011909.
[5] R. Ishizaki, T. Shinba, G. Mugishima, H. Haraguchi, M. Inoue, Time-series analysis of sleep-wake stage of rat EEG using time-dependent pattern entropy, Physica A 387 (2008) 3145.
[6] E. Núñez-Acosta, C. Lerma, M.F. Márquez, M.V. José, Mutual information analysis reveals bigeminy patterns in Andersen–Tawil syndrome and in subjects with a history of sudden cardiac death, Physica A 387 (2008) 3145.
[7] D.N.F. Fairbanks, S. Fujita, Snoring: an overview with historical perspectives, in: Snoring and Obstructive Sleep Apnea, Raven Press, New York, 1994.
[8] W.W. Flemons, Clinical practice. obstructive sleep apnea, N. Engl. J. Med 347 (7) (2002) 498–504.
[9] R.F. Drager, V.Y. Polotsky, G. Lorenzi-Filho, Obstructive sleep apnea: an emerging risk factor for atherosclerosis, Chest 140 (2011) 534–542.
[10] W.R. Ruehland, P.D. Rochford, F.J. O'Donoghue, R.J. Pierce, P. Singh, A.T. Thornton, The new aasm criteria for scoring hypopneas: impact on the apnea hypopnea index, Sleep 32 (2) (2009) 150–157.
[11] R.D. Chervin, Sleepiness, fatigue, tired, and lack of energy in obstructive sleep apnea, Chest 118 (2000) 372–379.
[12] N. Maimon, P.J. Hanly, Does snoring intensity correlate with the severity of obstructive sleep apnea? J. Clin. Sleep Med. 6 (5) (2010) 475–478.
[13] H. Ghaemmaghami, U.R. Abeyratne, C. Hukins, Normal probability testing of snore signals for diagnosis of obstructive sleep apnea, in: 31st Annual International Conference of the IEEE, 2009, pp. 5551–5554.
[14] A.K. Ng, T.S. Koh, U.R. Abeyratne, K. Puvanendran, Investigation of obstructive sleep apnea using nonlinear mode interactions in nonstationary snore signals, Ann. Biomed. Eng. 37 (9) (2009) 1796–1806.
[15] M. Cavusoglu, M. Kamasak, O. Erogul, T. Ciloglu, Y. Serinagaoglu, T. Akcam, An efficient method for snore/nonsnore classification of sleep sounds, Physiol. Meas. 28 (2007) 841.
[16] M. Cavusoglu, T. Ciloglu, Y. Serinagaoglu, M. Kamasak, O. Erogul, T. Akcam, Investigation of sequential properties of snoring episodes for obstructive sleep apnoea identification, Physiol. Meas. 29 (2008) 879.
[17] J. Lee, D. Kim, I. Kim, K.S. Park, S.I. Kim, Nonlinear analysis of human sleep EEG using detrended fluctuation analysis, Med. Eng. Phys. 26 (2004) 773.
[18] U. Rajendra Acharya, O. Faust, N. Kannathal, T. Chua, S. Laxminarayan, Non-linear analysis of EEG signals at various sleep stages, Comput. Methods Programs Biomed. 80 (2005) 37.
[19] J. Zhang, X. Yang, L. Luo, J. Shao, C. Zhang, J. Ma, G. Wang, Y. Liu, C. Peng, J. Fang, Assessing severity of obstructive sleep apnea by fractal dimension sequence analysis of sleep EEG, Physica A 388 (2009) 4407.
[20] A.P. Vieira, E.P. de Moura, L.L. Gonçalves, Fluctuation analyses for pattern classification in nondestructive materials inspection, EURASIP J. Adv. Signal Process. 2010 (14) (2010) 262869.
[21] J. Feder, Fractals, Plenum Press, New York, 1988.
[22] A.L. Goldberger, L.A.N. Amaral, J.M. Hausdorff, P.C. Ivanov, C.-K. Peng, H.E. Stanley, Fractal dynamics in physiology: alterations with disease and aging, Proc. Natl. Acad. Sci. USA 99 (Suppl. 1) (2002) 2466–2472. http://dx.doi.org/10.1073/pnas.012579499.
[23] J.M. Hausdorff, A. Lertratanakul, M.E. Cudkowicz, A.L. Peterson, D. Kaliton, A.L. Goldberger, Dynamic markers of altered gait rhythm in amyotrophic lateral sclerosis, J. Appl. Physiol. 88 (6) (2000) 2045–2053.
[24] R.C. Hwa, T.C. Ferree, Scaling properties of fluctuations in the human electroencephalogram, Phys. Rev. E 66 (2002) 021901.
[25] C.K. Peng, J.E. Mietus, Y.H. Liu, C. Lee, J.M. Hausdorff, H.E. Stanley, A.L. Goldberger, L.A. Lipsitz, Quantifying fractal dynamics of human respiration: age and gender effects, Ann. Biomed. Eng. 30 (5) (2002) 683–692.
[26] A.R. Webb, Statistical Pattern Recognition, second ed., John Wiley & Sons, Chichester, 2002.
[27] D. Pevernagie, R.M. Aarts, M. De Meyer, The acoustics of snoring, Sleep Med. Rev. 14 (2010) 131–144.